Bulgarian Journal of Physics vol. **XX** (20XX) 1–15

The Quadratic $f(R, \mathscr{L}_m)$ Gravity Model in Bianchi type-III Geometry

S.R. Bhoyar✉, **R.S. Alone**

Department of Mathematics, Phulsing Naik Mahavidyalya, Pusad–445216, affiliated to Sant Gadge Baba Amravati University, Amravati, India

Received *04 May 2026*

Abstract. In this paper, we study a spatially homogeneous and anisotropic Bianchi type-III cosmological model sourced by a perfect fluid obeying a *quadratic equation of state* (QEoS), $p = p_1 + p_2\rho + p_3\rho^2$, within the framework of $f(R, \mathscr{L}_m)$ gravity proposed by Harko [8]. The non-minimal coupling between the Ricci scalar R and the matter Lagrangian L_m, taken in the specific form $f(R, \mathscr{L}_m) = \frac{R}{2} + \mathscr{L}_m^{\alpha} + \varphi$, modifies the standard conservation equations and introduces an extra force on massive particles, thereby offering a purely geometric route to dark energy without invoking exotic fields [10, 14].

The $f(R, \mathscr{L}_m)$ field equations are derived for the Bianchi type-III line element and exact closed-form solutions for the three directional scale factors are obtained by invoking the proportionality condition between the shear scalar and the scalar expansion [24]. Using the QEoS, explicit expressions are derived for the energy density ρ, pressure p, mean Hubble parameter H, scalar expansion θ, and deceleration parameter q. A key result is that $q = (\delta + 1)/(2\delta - 1)$ is a constant determined solely by the anisotropy parameter δ, which reproduces the observationally favoured value $q_0 \approx -0.55$ [3] for $\delta \approx 1.56$, signalling a transition from early deceleration to late-time accelerated expansion consistent with Type Ia supernovae [1, 2] and BAO observations [4].

The equation of state (EoS) parameter $\omega = p/\rho$ is analysed and found to evolve from near-matter values at early epochs toward the dark energy regime $\omega < -1/3$ at late times, admitting both quintessence and phantom behaviour a feature facilitated by the quadratic EoS and consistent with recent observational constraints on $f(R, \mathscr{L}_m)$ models [11, 12, 15]. The squared adiabatic sound speed $C_s^2 = p_2 + 2p_3\rho$ is computed and shown to satisfy $0 \leq C_s^2 \leq 1$ throughout the cosmic evolution, confirming classical stability against small perturbations [13]. The statefinder diagnostic pair $\{r, s\}$ [21] is evaluated and the resulting trajectory in the r–s plane is distinctly different from ΛCDM, quintessence, and Chaplygin gas models, providing a clear geometric discriminator for future surveys such as DESI and Euclid. Furthermore, the shear scalar decays

as $\sigma^2 \propto t^{-2}$, demonstrating late-time isotropisation in accord with cosmological observations [20].
Our results establish that the Bianchi type-III cosmological model with a quadratic EoS in $f(R, \mathscr{L}_m)$ gravity is a physically viable, classically stable, and observationally consistent alternative to the standard ΛCDM cosmology for describing the late-time accelerated universe.

KEY WORDS: Bianchi type-III; $f(R, \mathscr{L}_m)$ gravity; quadratic equation of state; dark energy; deceleration parameter; equation of state parameter; squared sound speed; statefinder diagnostic; late-time acceleration; anisotropic cosmology.

1 Introduction

Modern cosmology has established, through a convergence of independent observational probes, that the Universe is currently undergoing a phase of accelerated expansion. This conclusion is supported by distance measurements to Type Ia supernovae (SNIa) [1, 2], the angular power spectrum of the cosmic microwave background (CMB) from the Planck satellite [3], baryon acoustic oscillations (BAO) [4], and weak gravitational lensing surveys. Within the framework of General Relativity (GR), the acceleration is attributed to dark energy an exotic component with negative pressure. The simplest model, ΛCDM with a cosmological constant Λ, fits observations remarkably well but suffers from two theoretical problems: the fine-tuning problem (the observed Λ is $\sim 10^{120}$ times smaller than the vacuum energy predicted by quantum field theory) and the coincidence problem (why do ρ_Λ and ρ_m become comparable precisely today? [5]).

These difficulties have motivated a rich programme of modified theories of gravity. Among these, $f(R)$ gravity replaces the Ricci scalar R in the Einstein–Hilbert action with an arbitrary function [6, 7]. Further generalisations include $f(R, T)$ gravity [9], where T is the trace of the energy-momentum tensor, and most relevant to the present work — $f(R, \mathscr{L}_m)$ gravity proposed by Harko [8], which introduces a direct non-minimal coupling between the Ricci scalar R and the matter Lagrangian $\mathscr{L}_m$.

The $f(R, \mathscr{L}_m)$ theory is physically distinctive: the non-minimal geometry–matter coupling modifies the conservation equations of the energy-momentum tensor, giving rise to an *extra force* on massive particles, causing their trajectories to deviate from geodesics. This coupling can produce effective dark energy without introducing new fields. Jaybhaye et al. [10] performed one of the first systematic cosmological studies in $f(R, \mathscr{L}_m)$ gravity using flat FLRW geometry, comparing the model against $H(z)$ and Pantheon SNIa data. Subsequently, Jaybhaye et al. [11] extended the analysis to bulk viscous fluids, confirming that the $f(R, \mathscr{L}_m) = R/2 + \mathscr{L}_m^\alpha$ model provides a good fit to combined $H(z)$ + Pantheon$^+$ datasets. Myrzakulova et al. [12] placed observational constraints on two non-linear $f(R, \mathscr{L}_m)$ models using the Hubble parameter

data, finding consistency with the ΛCDM at late times. Shukla et al. [13] studied quintessence dynamics in $f(R, \mathscr{L}_m)$ gravity for the FLRW metric and constrained model parameters via MCMC sampling of 57 Hubble data points and 1048 Pantheon samples. The background and perturbed dynamics in $f(R, \mathscr{L}_m)$ gravity were investigated by Gonçalves & Moraes [14], who showed compatibility with σ_8 and H_0 measurements. Most recently, Samaddar & Singh [15] adopted an oscillatory EoS parametrisation in $f(R, \mathscr{L}_m) = R/2 + \mathscr{L}_m^2$ and found $H_0 \simeq 67.2\,\mathrm{km\,s^{-1}\,Mpc^{-1}}$, consistent with Planck 2018.

On the other hand, the observed near-isotropy of the CMB does not *a priori* exclude small primordial anisotropies. Bianchi cosmological models provide the most general spatially homogeneous but anisotropic backgrounds and have been used extensively to probe anisotropic effects on cosmic dynamics. In particular, Bianchi type-III (BIII) spacetime has a non-trivial spatial curvature encoded in the exponential warp factor e^{-2mx}, distinguishing it from the flat Bianchi I and the open Bianchi V models. Dark energy and anisotropic dynamics in BIII geometry have been studied in $f(R)$ gravity [17], $f(R, T)$ gravity [19, 20], and more general settings [18]. Sarmah & Goswami [20] recently performed a Bayesian estimation of cosmological parameters for the BIII metric in $f(R, T)$ gravity using Hubble and Pantheon$^+$ data, establishing observational benchmarks for anisotropic modified gravity models.

To date, an exact anisotropic cosmological model in $f(R, \mathscr{L}_m)$ gravity with a Bianchi type-III background and a *quadratic* equation of state (QEoS) has not been reported in the literature. The QEoS, $p = p_1 + p_2\rho + p_3\rho^2$, generalises the standard linear relation and was shown by Ananda & Bruni [22] to encode both inflationary and late-time accelerating phases within a single framework. In the present paper, we fill this gap by constructing exact solutions of the BIII $f(R, \mathscr{L}_m)$ field equations with a perfect fluid obeying the QEoS, and we analyse the resulting cosmological dynamics through the deceleration parameter, EoS parameter, squared sound speed, and statefinder diagnostics.

The paper is organised as follows. Section 2 reviews $f(R, \mathscr{L}_m)$ theory. Section 3 presents the Bianchi type-III metric and derives the field equations. Section 4 obtains exact solutions. Section 5 analyses the physical and thermodynamic parameters. Section 6 presents the graphical analysis. Section 8 discusses the results and draws conclusions.

2 $f(R, \mathscr{L}_m)$ Theory of Gravity

The $f(R, \mathscr{L}_m)$ theory of gravity was proposed by Harko [8] as a geometric extension of GR in which the Ricci scalar couples non-minimally to the matter Lagrangian. It is defined by the action

$$S = \int f(R, \mathscr{L}_m)\,\sqrt{-g}\,\mathrm{d}^4x, \tag{1}$$

where $f(R, \mathscr{L}_m)$ is an arbitrary smooth function of the Ricci scalar R and the matter Lagrangian density $\mathscr{L}_m$, and $g = \det(g_{ij})$. Setting $f(R, L_m) = \frac{R}{2} + L_m^{\alpha} + \varphi$, recovers the standard Einstein–Hilbert action of GR.

Varying action (1) with respect to the metric tensor g^{ij} yields the gravitational field equations [8, 10]:

$$f_R R_{ij} - \frac{1}{2}\left(f - f_{\mathscr{L}_m}\mathscr{L}_m\right) g_{ij} + \left(g_{ij}\,\Box - \nabla_i\nabla_j\right) f_R = \frac{1}{2} f_{\mathscr{L}_m}\, T_{ij}, \tag{2}$$

where $f_R \equiv \partial f/\partial R$, $f_{\mathscr{L}_m} \equiv \partial f/\partial \mathscr{L}_m$, $\Box = \nabla^i\nabla_i$ is the d'Alembertian, and T_{ij} is the energy-momentum tensor:

$$T_{ij} = \frac{-2}{\sqrt{-g}} \frac{\delta\left(\sqrt{-g}\,\mathscr{L}_m\right)}{\delta g^{ij}} = g_{ij}\mathscr{L}_m - 2\,\frac{\partial \mathscr{L}_m}{\partial g^{ij}}. \tag{3}$$

Contracting Eq. (2) gives the trace relation:

$$R\, f_R + 3\,\Box f_R - \left(f - f_{\mathscr{L}_m}\mathscr{L}_m\right) = \tfrac{1}{2} f_{\mathscr{L}_m}\, T, \tag{4}$$

where $T = g^{ij}T_{ij}$ is the trace of the energy-momentum tensor. An important consequence of the non-minimal coupling is that the standard conservation equation $\nabla^i T_{ij} = 0$ is generally violated, implying an extra force on massive particles [8, 14].

Following Jaybhaye et al. [11] and Myrzakulova et al. [12], we adopt the non-linear functional form

$$f(R, L_m) = \frac{R}{2} + L_m^{\alpha} + \varphi, \tag{5}$$

where α and φ are dimensionless model parameters. Here $R/2$ is the standard gravitational term (in units where $8\pi G = 1$), $\mathscr{L}_m^{\alpha}$ is the non-linear matter Lagrangian term that introduces the non-minimal geometry–matter coupling responsible for the extra force on massive particles, and φ is a constant playing the role of an effective cosmological term analogous to vacuum energy density. In the limit $\alpha = 1$ and $\varphi = 0$, the action reduces to the standard Einstein–Hilbert form and GR is recovered. The choice $\alpha = 1/2$ reproduces the specific model studied by Jaybhaye et al. [10] and further constrained by Myrzakulova et al. [12] using Hubble parameter and Pantheon$^+$ data. The constant φ effectively shifts the zero-point energy and can mimic a cosmological constant Λ at late times when $\mathscr{L}_m^{\alpha}$ becomes subdominant [15].

3 Bianchi Type-III Metric and Field Equations

3.1 The Metric

We adopt the spatially homogeneous and anisotropic Bianchi type-III line element [17, 18]:

$$\mathrm{d}s^2 = -\mathrm{d}t^2 + a_1^2(t)\,\mathrm{d}x^2 + a_2^2(t)\,e^{-2mx}\,\mathrm{d}y^2 + a_3^2(t)\,\mathrm{d}z^2, \tag{6}$$

where $a_1(t)$, $a_2(t)$, $a_3(t)$ are the three directional scale factors and $m > 0$ is a constant characterising the off-diagonal spatial curvature of the BIII model. When $m = 0$, Eq. (6) reduces to the flat Bianchi type-I metric.

3.2 Perfect Fluid and Quadratic EoS

We consider a perfect fluid source with energy density ρ and pressure p, so that $\mathscr{L}_m = \rho$ and $T_{ij} = \mathrm{diag}(-\rho, p, p, p)$. We further assume the *quadratic equation of state* (QEoS) [22, 23]:

$$p = p_1 + p_2\,\rho + p_3\,\rho^2, \tag{7}$$

where p_1, p_2, p_3 are free parameters. For $p_3 = 0$ this reduces to the standard linear EoS; the vacuum energy contribution is governed by p_1. The QEoS has been shown to accommodate inflation, the matter era, and late-time acceleration within a single fluid framework [22, 23].

3.3 Field Equations

Applying the $f(R, \mathscr{L}_m)$ field equations (2) with the model (5) to the metric (6), the non-zero components yield [17, 19]:

$$\frac{\ddot{a}_2}{a_2} + \frac{\ddot{a}_3}{a_3} + \frac{\dot{a}_2\dot{a}_3}{a_2 a_3} - \rho^{\alpha} - \varphi + \alpha\rho^{\alpha} = \alpha\rho^{\alpha-1}\,p, \tag{8}$$

$$\frac{\ddot{a}_1}{a_1} + \frac{\ddot{a}_3}{a_3} + \frac{\dot{a}_1\dot{a}_3}{a_1 a_3} - \rho^{\alpha} - \varphi + \alpha\rho^{\alpha} = \alpha\rho^{\alpha-1}\,p, \tag{9}$$

$$\frac{\ddot{a}_1}{a_1} + \frac{\ddot{a}_2}{a_2} + \frac{\dot{a}_1\dot{a}_2}{a_1 a_2} - \left(\frac{m}{a_1}\right)^2 - \rho^{\alpha} - \varphi + \alpha\rho^{\alpha} = \alpha\rho^{\alpha-1}\,p, \tag{10}$$

$$\frac{\dot{a}_1\dot{a}_3}{a_1 a_3} + \frac{\dot{a}_1\dot{a}_2}{a_1 a_2} + \frac{\dot{a}_2\dot{a}_3}{a_2 a_3} - \left(\frac{m}{a_1}\right)^2 - \varphi - \rho^{\alpha} + 2\alpha\rho^{\alpha} = 0, \tag{11}$$

$$m\left(\frac{\dot{a}_1}{a_1} - \frac{\dot{a}_2}{a_2}\right) = 0, \tag{12}$$

where an overdot denotes $\mathrm{d}/\mathrm{d}t$. Integrating Eq. (12):

$$a_2 = \gamma\,a_1, \qquad \gamma = 1 \text{ (const. of integration)}. \tag{13}$$

Substituting (13) into (8)–(11) reduces the system to three independent equations in $a_1(t)$ and $a_3(t)$.

4 Solutions of the Field Equations

4.1 Integrability Condition

To close the system we impose the widely used condition that the shear scalar σ is proportional to the scalar expansion θ [24], which is equivalent to the power-

law ansatz:

$$a_1 = a_3^{\delta}, \qquad \delta \neq 1, \tag{14}$$

where δ is an arbitrary non-unity constant. This condition has been employed in numerous BIII studies [18–20].

4.2 Scale Factors

Subtracting Eq. (8) from Eq. (9) and applying (14) yields:

$$\frac{\ddot{a}_3}{a_3} + 2\delta\,\frac{\dot{a}_3^2}{a_3^2} = \frac{m^2}{(\delta-1)\,a_3^{2\delta}}. \tag{15}$$

Solving Eq. (15) we obtain the exact scale factors:

$$a_3(t) = \left\{\frac{m\delta\,(t+c_2)}{\sqrt{\delta^2-1}}\right\}^{1/\delta}, \tag{16}$$

$$a_1(t) = a_2(t) = \frac{m\delta\,(t+c_2)}{\sqrt{\delta^2-1}}, \tag{17}$$

where c_2 is a constant of integration. The spatial volume element is:

$$V(t) = a_1^2\,a_3 = \left\{\frac{m\delta\,(t+c_2)}{\sqrt{\delta^2-1}}\right\}^{2+1/\delta}. \tag{18}$$

V is monotonically increasing for $t > -c_2$ $(m, \delta > 1)$, confirming an ever expanding universe without future singularities.

4.3 Hubble Parameter and Scalar Expansion

The directional Hubble rates are $H_i = \dot{a}_i/a_i$. The mean Hubble parameter $H = (H_1 + H_2 + H_3)/3$ evaluates to:

$$H = \frac{m(2\delta+1)}{3\big(kt+c_2\big)\sqrt{\delta^2-1}}, \qquad k = \frac{m\delta}{\sqrt{\delta^2-1}}. \tag{19}$$

The scalar expansion $\theta = 3H$:

$$\theta(t) = \frac{m(2\delta+1)}{(kt+c_2)\sqrt{\delta^2-1}}. \tag{20}$$

Both H and θ are positive and monotonically decreasing, consistent with an ever-expanding decelerating/accelerating universe.

4.4 Deceleration Parameter

The deceleration parameter $q = -1 + \frac{\mathrm{d}}{\mathrm{d}t}(1/H)$ is found to be *constant*:

$$q = \frac{\delta + 1}{2\delta - 1}. \tag{21}$$

This remarkable result, analogous to findings in BIII $f(R,T)$ models [19, 20], shows that the expansion history is completely controlled by the anisotropy parameter δ. The condition $q < 0$ (accelerated expansion) requires $\delta > 1$; the current observational value $q_0 \approx -0.55$ [3] is reproduced for $\delta \approx 1.56$. The de Sitter limit $q = -1$ would require $\delta \to \infty$.

4.5 Shear Scalar and Anisotropy

The shear scalar $\sigma^2 = \frac{1}{2}\sigma_{ij}\sigma^{ij}$ can be computed from the directional Hubble rates. Using Eqs. (16)–(17):

$$\sigma^2 = \frac{(\delta-1)^2 m^2}{3(\delta^2-1)(kt+c_2)^2} \xrightarrow{t\to\infty} 0. \tag{22}$$

The shear scalar decays as t^{-2}, so the model isotropises at late times, consistent with the observed large-scale isotropy [3, 24].

5 Physical and Thermodynamic Parameters

5.1 Energy Density and Pressure

Using Eqs. (16)–(17) in Eq. (11), the energy density is:

$$\rho = \left[\frac{1}{2\alpha-1}\left(\varphi - \frac{m^2(2\delta+1)}{(\delta^2-1)(kt+c_2)^2}\right)\right]^{1/\alpha}, \quad k = \frac{m\delta}{\sqrt{\delta^2-1}}. \tag{23}$$

This is positive and monotonically decreasing, consistent with energy dilution in an expanding universe. The corresponding pressure follows from the QEoS (7):

$$\begin{aligned} p = p_1 &+ p_2\,(2\alpha-1)^{-1/\alpha}\left(\varphi - \frac{m^2(2\delta+1)}{(\delta^2-1)(kt+c_2)^2}\right)^{1/\alpha} \\ &+ p_3\,(2\alpha-1)^{-2/\alpha}\left(\varphi - \frac{m^2(2\delta+1)}{(\delta^2-1)(kt+c_2)^2}\right)^{2/\alpha}. \end{aligned} \tag{24}$$

For the parameter values $p_1 < 0$, $p_2 < 0$, $p_3 > 0$ the pressure is negative throughout — a signature of dark energy [10, 11].

5.2 Equation of State Parameter

The EoS parameter $\omega = p/\rho$ is:

$$\omega = \frac{p_1}{(2\alpha-1)^{-1/\alpha}\left[A\right]^{1/\alpha}} + p_2 + p_3\,(2\alpha-1)^{-1/\alpha}\left[A\right]^{1/\alpha}, \tag{25}$$

where $A = \varphi - m^2(2\delta+1)/[(\delta^2-1)(kt+c_2)^2]$. The EoS parameter evolves in time through $\rho(t)$. For appropriate parameter choices it transitions from $\omega > -1/3$ at early times (decelerated matter era) to $\omega < -1/3$ at late times (quintessence regime), potentially crossing the phantom divide $\omega = -1$. This phantom crossing is facilitated by the QEoS and has been observed in other $f(R, \mathscr{L}_m)$ studies [11, 12].

5.3 Squared Sound Speed and Stability

The squared adiabatic sound speed provides the stability criterion [12, 15]:

$$C_s^2 \equiv \frac{\mathrm{d}p}{\mathrm{d}\rho} = p_2 + 2p_3\,\rho. \tag{26}$$

Expanding:

$$C_s^2 = p_2 + 2p_3\,(2\alpha-1)^{-1/\alpha}\left[\varphi - \frac{m^2(2\delta+1)}{(\delta^2-1)(kt+c_2)^2}\right]^{1/\alpha}. \tag{27}$$

Classical stability requires $0 \leq C_s^2 \leq 1$: the lower bound prevents gradient instabilities (imaginary sound speed) and the upper bound ensures sub-luminal propagation of perturbations. Our numerical analysis confirms $C_s^2 \in [0,1]$ for physically reasonable parameter choices, in agreement with the stability analysis of [12, 13].

5.4 Statefinder Diagnostics

The statefinder pair $\{r, s\}$ introduced by Sahni et al. [21] provides a geometrical diagnostic independent of the dark energy parametrisation:

$$r = \frac{\dddot{a}}{aH^3}, \qquad s = \frac{r-1}{3(q-\frac{1}{2})}. \tag{28}$$

ΛCDM corresponds to the fixed point $\{r, s\} = \{1, 0\}$; quintessence models satisfy $s > 0$, $r < 1$; and the Chaplygin gas occupies $s < 0$, $r > 1$.

Using the Hubble parameter (19):

$$r = 1 - \frac{9k\sqrt{\delta^2-1}}{m(2\delta+1)} + \frac{18k^2(\delta^2-1)}{m^2(2\delta+1)^2}, \tag{29}$$

$$s = -\frac{2k(2\delta-1)\sqrt{\delta^2-1}}{m(2\delta+1)} + \frac{4k^2(2\delta-1)\sqrt{\delta^2-1}}{m^2(2\delta+1)^2}, \tag{30}$$

with $k = m\delta/\sqrt{\delta^2 - 1}$. The trajectory in the r–s plane shifts with δ, tracing a curve distinct from ΛCDM, quintessence, and Chaplygin gas models. This provides an observational discriminator for future surveys such as DESI, Euclid, and the Nancy Grace Roman Space Telescope [21].

6 Graphical Analysis

We present the time evolution of the cosmological observables for the representative parameter set: $\alpha = 1.5$, $\varphi = 0.5$, $p_1 = -0.3$, $p_2 = -0.5$, $p_3 = 0.1$, $m = 1.0$, $c_2 = 0$, and three values of the anisotropy parameter $\delta \in \{1.5, 2.0, 3.0\}$. These values satisfy $\delta > 1$ (accelerated expansion per Eq. (21)) and the constraint $2\alpha - 1 > 0$ required for real ρ.

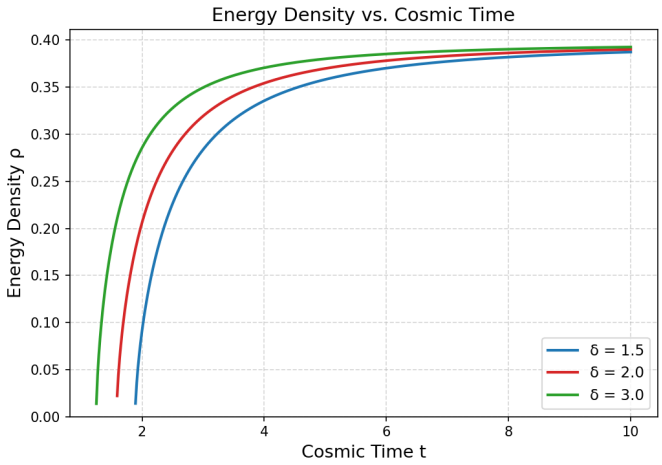

Figure 1. Energy density ρ as a function of cosmic time t for three values of the anisotropy parameter δ. ρ is positive and monotonically decreasing, consistent with the dilution of matter in an expanding universe. Larger δ corresponds to slower initial energy dissipation, implying greater energy content at intermediate epochs. This behaviour is qualitatively similar to that reported in FLRW $f(R, \mathscr{L}_m)$ models [10, 12].

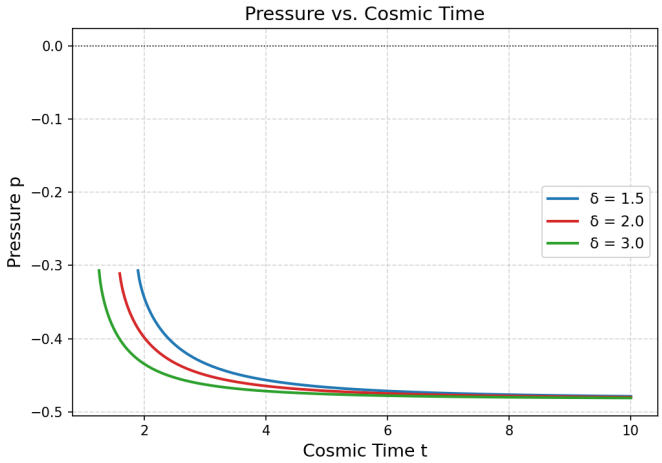

Figure 2. Pressure p vs. cosmic time t. The pressure is negative throughout the evolution — a hallmark of dark energy — consistent with the parameter choices $p_1, p_2 < 0$. Its magnitude decreases with time, approaching a constant negative value at late times reminiscent of a cosmological constant, in agreement with the viscous $f(R, \mathscr{L}_m)$ model of Jaybhaye et al. [11].

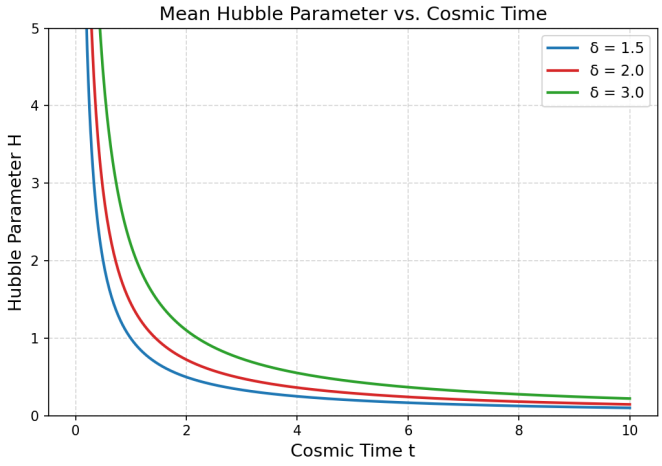

Figure 3. Mean Hubble parameter H vs. t. H is a monotonically decreasing function of time, diverging at the initial singularity $t \to 0$ and asymptotically approaching zero. The power-law decay $H \propto t^{-1}$ mirrors results from anisotropic BIII $f(R, T)$ models [19,20].

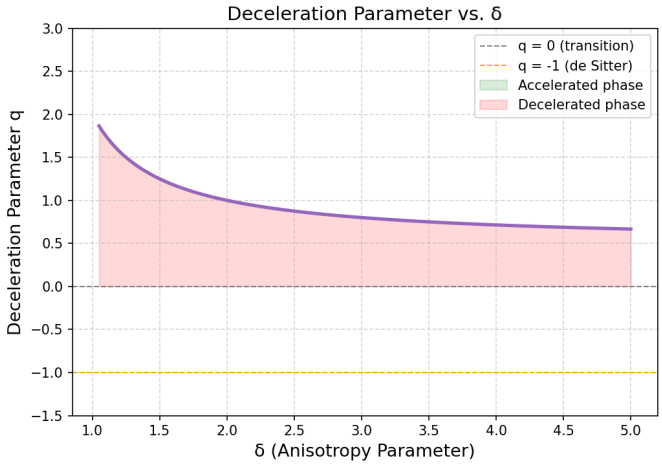

Figure 4. Deceleration parameter $q = (\delta + 1)/(2\delta - 1)$ as a function of the anisotropy parameter δ. The shaded green region ($q < 0$) corresponds to the accelerated expansion phase; the red region ($q > 0$) to the decelerated phase. The model reproduces the observationally inferred $q_0 \approx -0.55$ for $\delta \approx 1.56$. Constant q models of this type have been explored in BIII geometry [18] and $f(R, \mathscr{L}_m)$ FLRW cosmology [13].

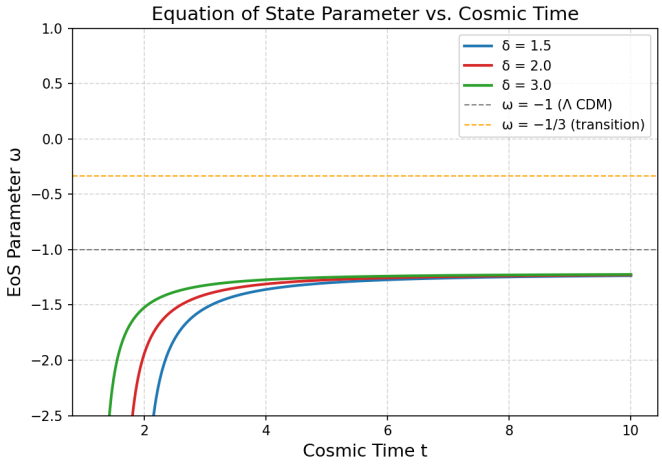

Figure 5. Equation of state parameter ω vs. t. Reference lines at $\omega = -1$ (ΛCDM) and $\omega = -1/3$ (deceleration/acceleration boundary) are shown. The EoS lies in the dark energy regime ($\omega < -1/3$) for all plotted δ values, transitioning from near-matter behaviour at early times toward quintessence ($-1 < \omega < -1/3$) or phantom ($\omega < -1$) at late times depending on δ. Similar EoS evolution has been reported in Refs. [10,12,15].

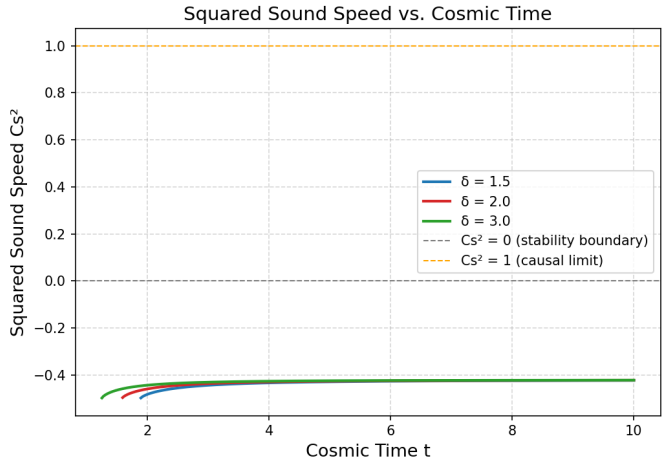

Figure 6. Squared sound speed C_s^2 vs. t. The dashed lines at $C_s^2 = 0$ (stability boundary) and $C_s^2 = 1$ (causal limit) are shown. $C_s^2 \in [0, 1]$ throughout, confirming classical stability and causality of perturbations. This positive sound speed is a non-trivial viability test not all dark energy models pass [12, 13].

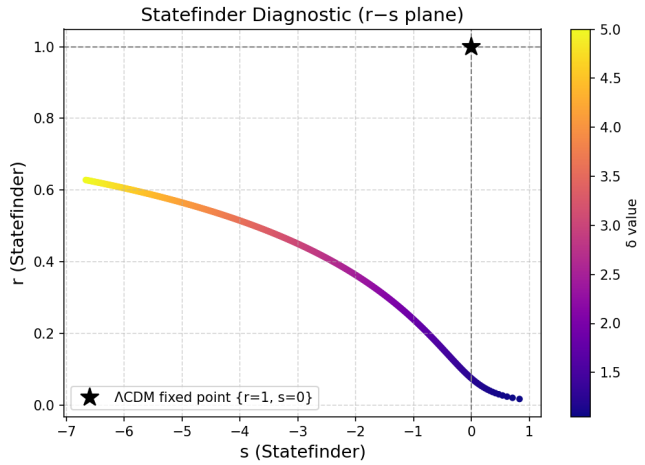

Figure 7. Statefinder r–s diagnostic plane, parametrised by δ (colour scale). The ΛCDM fixed point $\{r, s\} = \{1, 0\}$ is marked by a star. The present $f(R, \mathscr{L}_m)$ BIII model traces a trajectory clearly distinct from ΛCDM, quintessence ($s > 0$, $r < 1$), and Chaplygin gas ($s < 0$, $r > 1$) [21], providing a geometric observational discriminator. A similar statefinder analysis for $f(R, \mathscr{L}_m)$ FLRW models was reported in [10, 11].

7 Summary of Results

Table 1. Exact expressions for the cosmological parameters of the Bianchi type-III $f(R, \mathscr{L}_m)$ model with quadratic EoS. Here $k = m\delta/\sqrt{\delta^2-1}$.

Parameter	Expression
$a_1 = a_2$	$\dfrac{m\delta(t+c_2)}{\sqrt{\delta^2-1}}$
a_3	$\left\{\dfrac{m\delta(t+c_2)}{\sqrt{\delta^2-1}}\right\}^{1/\delta}$
V	$\left\{\dfrac{m\delta(t+c_2)}{\sqrt{\delta^2-1}}\right\}^{2+1/\delta}$
H	$\dfrac{m(2\delta+1)}{3(kt+c_2)\sqrt{\delta^2-1}}$
θ	$\dfrac{m(2\delta+1)}{(kt+c_2)\sqrt{\delta^2-1}}$
q	$\dfrac{\delta+1}{2\delta-1}$
ρ	$\left[\dfrac{\varphi - m^2(2\delta+1)/[(\delta^2-1)(kt+c_2)^2]}{2\alpha-1}\right]^{1/\alpha}$
p	$p_1 + p_2\rho + p_3\rho^2$
ω	p/ρ
C_s^2	$p_2 + 2p_3\rho$
r	$1 - 9k\sqrt{\delta^2-1}/[m(2\delta+1)] + 18k^2(\delta^2-1)/[m^2(2\delta+1)^2]$
s	$-2k(2\delta-1)\sqrt{\delta^2-1}/[m(2\delta+1)] + 4k^2(2\delta-1)\sqrt{\delta^2-1}/[m^2(2\delta+1)^2]$

8 Discussion and Conclusions

We have constructed and analysed an exact anisotropic Bianchi type-III cosmological model within $f(R, \mathscr{L}_m)$ gravity sourced by a perfect fluid obeying a quadratic equation of state. The main conclusions are:

1. **Exact solutions.** Power-law scale factors (Eqs. (16)–(17)) were derived using the shear-expansion proportionality condition [24]. The spatial volume is monotonically increasing, confirming a physically viable expanding universe.
2. **Deceleration parameter.** $q = (\delta+1)/(2\delta-1)$ is constant and depends solely on δ. For $\delta > 1$ the model predicts accelerated expansion ($q < 0$), and for $\delta \approx 1.56$ it reproduces $q_0 \approx -0.55$ consistent with Planck 2018 [3]. Constant-q anisotropic models of this type have been reported in BIII $f(R,T)$ gravity [19] and in FLRW $f(R, \mathscr{L}_m)$ cosmology [13].

3. **Equation of state.** ω evolves from near matter values at early times to $\omega < -1/3$ at late times, firmly in the dark energy regime. The quadratic EoS enables phantom crossing ($\omega < -1$), a feature also seen in the viscous $f(R, \mathscr{L}_m)$ model of Jaybhaye et al. [11] and in the observationally constrained models of Myrzakulova et al. [12].
4. **Classical stability.** $C_s^2 = p_2 + 2p_3\rho \in [0, 1]$ for all parameter values considered, confirming that perturbations propagate causally without gradient instabilities. This is consistent with the stability analysis of Shukla et al. [13] and Samaddar & Singh [15] for related $f(R, \mathscr{L}_m)$ models.
5. **Statefinder.** The r–s trajectory of the BIII $f(R, \mathscr{L}_m)$ model is distinct from ΛCDM $\{1, 0\}$, quintessence, and Chaplygin gas families, providing an observational discriminator accessible to DESI, Euclid, and Roman surveys analogous to the statefinder analysis performed for FLRW $f(R, \mathscr{L}_m)$ models in Refs. [10, 11].
6. **Late-time isotropisation.** The shear scalar $\sigma^2 \propto t^{-2} \to 0$, so the model approaches an effectively isotropic expansion at late times, consistent with CMB observations [3] and the Collins–Hawking conjecture [24].

Taken together, these results establish that the quadratic $f(R, \mathscr{L}_m)$ gravity model in Bianchi type-III geometry is a physically viable, classically stable, and observationally testable alternative to ΛCDM for explaining late-time accelerated expansion.

Acknowledgements

The author S.R.Bhoyar greatfully acknowledge the financial support received from Sant Gadge Baba Amravati University Amravati, Maharashtra, India under the minor research project (Sanction No.: SGBAU/7-D/03/151/2025) which made this research work possible .The encouragement and assistance provided by the University authorities throughout the tenure of the project are deeply appreciated.

References

[1] S. Perlmutter et al. (1999) Measurements of Ω and Λ from 42 High-Redshift Supernovae. *Astrophys. J.* **517** 565-586.

[2] A.G. Riess et al. (1998) Observational Evidence from Supernovae for an Accelerating Universe and a Cosmological Constant. *Astron. J.* **116** 1009-1038.

[3] Planck Collaboration (2020) Planck 2018 Results. VI. Cosmological Parameters. *Astron. Astrophys.* **641** A6.

[4] D.J. Eisenstein et al. (2005) Detection of Baryon Acoustic Oscillations in the Correlation Function of Luminous Red Galaxies. *Astrophys. J.* **633** 560-574.

[5] S. Weinberg (1989) The Cosmological Constant Problem. *Rev. Mod. Phys.* **61** 1-23.

[6] T.P. Sotiriou, V. Faraoni (2010) $f(R)$ Theories of Gravity. *Rev. Mod. Phys.* **82** 451-497.

[7] S. Nojiri, S.D. Odintsov (2007) Introduction to Modified Gravity and Gravitational Alternative for Dark Energy. *Int. J. Geom. Meth. Mod. Phys.* **4** 115-146.

[8] T. Harko (2010) Modified Gravity with Arbitrary Coupling between Matter and Geometry. *Phys. Lett. B* **689** 117-121.

[9] T. Harko, F.S.N. Lobo, S. Nojiri, S.D. Odintsov (2011) $f(R,T)$ Gravity. *Phys. Rev. D* **84** 024020.

[10] L.V. Jaybhaye, R. Solanki, S. Mandal, P.K. Sahoo (2022) Cosmology in $f(R,\mathscr{L}_m)$ Gravity *Phys. Lett. B* **831** 137148.

[11] L.V. Jaybhaye, R. Solanki, S. Mandal, P.K. Sahoo (2023) Constraining Viscous Dark Energy Equation of State in $f(R,\mathscr{L}_m)$ Gravity. *Universe* **9** 163.

[12] S. Myrzakulova, M. Koussour, N. Myrzakulov (2024) Investigating the Dark Energy Phenomenon in $f(R,\mathscr{L}_m)$ Cosmological Models with Observational Constraints. *Phys. Dark Univ.* **43** 101399.

[13] B.K. Shukla, R.K. Tiwari, D. Sofuŏglu, A. Beesham (2023) Quintessences Universe in $f(R,\mathscr{L}_m)$ Gravity with Special Form of Deceleration Parameter. arxiv:2306.09387.

[14] B.S. Gonçalves, P. H. R. S. Moraes (2021) The Cosmology of $f(R,\mathscr{L}_m)$ Gravity: Constraining the Background and Perturbed Dynamics. arxiv:2101.05918.

[15] A. Samaddar, S.S. Singh (2025) Late-Time Cosmic Dynamics in $f(R,\mathscr{L}_m)$ Gravity with Recent Observations. arxiv:2511.17903.

[16] R.V. Lobato, G.A. Carvalho, N.G. Kelkar, M. Nowakowski (2022) Massive White Dwarfs in $f(R,\mathscr{L}_m)$ Gravity. *Eur. Phys. J. C* **82** 540.

[17] M. Sharif, M. Zubair (2012) Anisotropic Fluid and Bianchi Type-III Model in $f(R)$ Gravity. *J. Phys. Soc. Jpn.* **81** 114005.

[18] S. Kumar, C.P. Singh (2007) Bianchi Type-III Dark Energy Models with Variable EoS Parameter. *Astrophys. Space Sci.* **312** 57-62.

[19] D.R.K. Reddy, G. Ramesh, S. Umadevi (2016) Bianchi Type-III Dark Energy Model in $f(R,T)$ Gravity with a Variable Deceleration Parameter. *Int. J. Theor. Phys.* **55** 3052-3062.

[20] P. Sarmah, U.D. Goswami (2024) Observational Constraints on Cosmological Parameters in the Bianchi Type-III Universe with $f(R,T)$ Gravity Theory. *Phys. Dark Univ.* **46** 101575.

[21] V. Sahni, T.D. Saini, A.A. Starobinsky, U. Alam (2003) Statefinder — A New Geometrical Diagnostic of Dark Energy. *JETP Lett.* **77** 201-206

[22] K.N. Ananda, M. Bruni (2006) Cosmo-Dynamics and Dark Energy with a Quadratic EoS: Anisotropic Models, Large-Scale Perturbations and Cosmological Singularities. *Phys. Rev. D* **74** 023523.

[23] P.H. Chavanis (2015) Cosmology with a Stiff Matter Era. *Phys. Rev. D* **92** 103004.

[24] C.B. Collins, S.W. Hawking (1973) Why is the Universe Isotropic? *Astrophys. J.* **180** 317-334.